Electronic Materials Letters (2024) 20:192–198
https://doi.org/10.1007/s13391-023-00439-y

ORIGINAL ARTICLE – NANOMATERIALS

Characteristics of Rhombohedral (3R) Structure of α-In_2Se_3 Nanosheets by Mechanical Exfoliation

Dong Hyun Seo[1] · Ju Won Kim[1] · Jin-Hoo Seong[1,3] · Hyo-Chang Lee[4,5] · Sang-il Kim[2] · TaeWan Kim[1]

Received: 6 February 2023 / Accepted: 1 May 2023 / Published online: 5 June 2023

Abstract

The mechanically exfoliated ultrathin 3R α-In_2Se_3 nanosheets were transferred onto a SiO_2/Si substrate. Using atomic force microscopy, it was confirmed that the transferred α-In_2Se_3 transferred had a thickness of 15–120 nm. The thickness-dependence of Raman peaks of E^2, A_1^1, E^4, and A_1^2 was observed from the Raman spectra. Moreover, the measured photoluminescence peak values in the range of 869–895 nm indicate a blue shift as the thickness decreases. The field-effect transistor based on α-In_2Se_3 exhibited an n-type semiconductor behavior. From the transfer curve at gate voltage of 10 V, the derived values of the mobility and ON/OFF ratio are 24.26 $cm^2 V^{-1} s^{-1}$ and 1.84, respectively. In addition, it was confirmed that the 3R α-In_2Se_3 layers had a high photoresponsivity of up to approximately 34,500 A/W under illumination ($\lambda = 750$ nm).

Graphical abstract

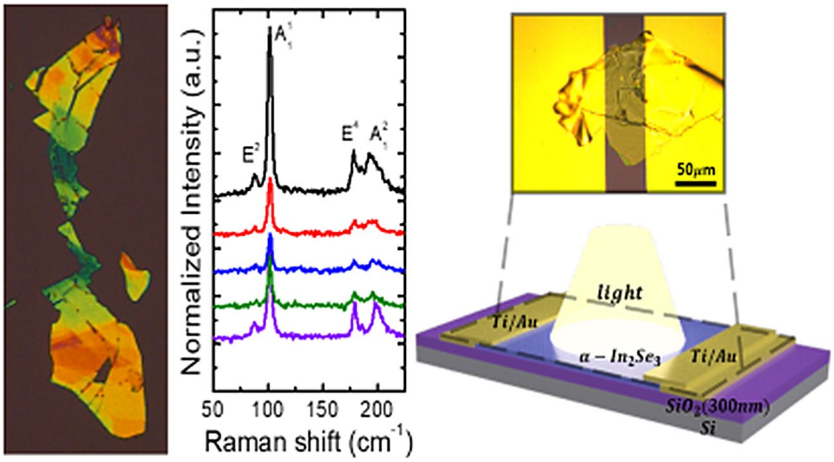

Keywords Rhombohedral α-In_2Se_3 nanosheets · Raman spectra · Photoluminescence spectra · Electrical properties · Photoresponsivity

---

✉ Sang-il Kim
sang1.kim@uos.ac.kr

✉ TaeWan Kim
twkim@jbnu.ac.kr

[1] Department of Electrical Engineering and Smart Grid Research Center, Jeonbuk National University, Jeonju 54896, South Korea

[2] Department of Materials Science and Engineering, University of Seoul, Seoul 02504, South Korea

[3] Advanced Instrumentation Institute, Korea Research Institute of Standards and Science (KRISS), Daejeon 34113, South Korea

[4] School of Electronics and Computer Engineering, Korea Aerospace University, Goyang 10540, South Korea

[5] Department of Semiconductor Science, Engineering and Technology, Korea Aerospace University, Goyang 10540, South Korea

1 Introduction

Since the discovery of graphene, two-dimensional (2D) materials have recently received considerable attention owing to their electrical and optoelectronic properties. 2D materials are obtained by reducing the lateral dimensions of bulk materials to extremely small atomic layers. Compared to bulk materials, several 2D materials, including transition metal dichalcogenides (TMDs), exhibit significantly different band structure changes [1, 2]. TMDs have been studied extensively, whereas non-TMDs have been neglected. Non-transition metal dichalcogenides, such as In_xSe_y, Sb_2Te_3 and Bi_2Te_3 exhibit various types of phases depending on the temperature or pressure [3–5]. In_2Se_3 is an interesting III–VI semiconductor among non-transition metal dichalcogenides owing to its various phases and excellent optical properties [6]. In_2Se_3 possesses five known crystal structures and phases ($\alpha, \beta, \gamma, \delta$ *and* κ) that depend on the temperature [7, 8]. The layers of α-In_2Se_3 are stacked together through van der Waals interactions. There are two structures of α-In_2Se_3 characterized by the number of stacked layers in the unit cell: hexagonal (2H), which has two stacked layers, and rhombohedral (3R), which has three [9, 10]. The Raman spectrum can be used to distinguish between these two structures. $90\,cm^{-1}(E^2)$, one of the Raman peak values of α-In_2Se_3, is clearly visible in the hexagonal structure but is less prominent in the rhombohedral structure [10]. Owing to its high photosensivity, fast photoresponse, significant conductivity, and outstanding optical transmission, α-In_2Se_3 has a bandgap of 1.43 eV and has various applications including photosensors, photodetectors and solar cells [11, 12]. In addition, α-In_2Se_3 as a ferroelectric material, exhibits spontaneous polarization in the absence of an external electric field. Thus, α-In_2Se_3 can be applied to ferroelectric semiconductor field-effect transistors [13]. However, despite many studies on the optical and optoelectronic properties of 2H structures of α-In_2Se_3, 3R structures have not been much explored [6, 10, 18]. In this work, we identified the optical properties of 3R α-In_2Se_3 by measuring the Raman and photoluminescence (PL) spectra. In particular, a 3R α-In_2Se_3–based phototransistor was fabricated and its optoelectronic properties were measured.

2 Experiment

Because the 3R α-In_2Se_3 flake has a weak bond between the atoms owing to van der Waals forces, it can be exfoliated while maintaining its two-dimensional structure using the adhesive force of a tape. 3R α-In_2Se_3 was mechanically exfoliated and transferred onto a SiO_2/Si substrate. We confirmed the surface shape and thickness of the sample flakes of 3R α-In_2Se_3 through an optical microscope (OM) and an atomic force microscope (AFM), respectively, at the Center for University-Wide Research Facilities, Jeonbuk National University. Structural identification of the 3R α-In_2Se_3 powder was performed using X-ray diffraction (XRD, D8 Discover, Bruker) at 40 kV and 40 mA. Cu Kα radiation (λ = 1.5406 Å) and a scan rate of 0.02° sec^{-1} were used to record patterns ranging from 10° to 70°. Subsequently, the Raman spectrum and PL were measured and analyzed using FEX (NOST) at the National NanoFAB Center (NNFC) to determine the optical properties of 3R α-In_2Se_3. For measuring the Raman spectra, the laser wavelength and its intensity were set to 532 nm and 2.878 mW, respectively. The same laser wavelength was used for the PL measurements. For measuring the PL intensity mapping, the laser wavelength was set to 514 nm, and the area of $10 \times 10\,\mu m$ and 121 points were measured at the KAIST Analysis Center for Research Advancement (KARA). The experiments were conducted at 300 K. The 3R α-In_2Se_3-based field effect transistor (FET) bar pattern was manufactured using copper wires to define the dimensions of the channel, and Ti/Au (5/50 nm) was deposited using an electron beam evaporator in the uncovered areas. The thickness of the sample flakes of 3R α-In_2Se_3-based FET was measured by a surface profiler (Tencor P-7 Stylus Profiler, KLA Corporation) at Korea Research Institute of Standards and Science (KRISS). All optoelectrical measurements were performed using a four-point probe station (M6VC, MS-tech) with a commercial parameter analyzer (4200, Keithley Inc.) under vacuum conditions of 10^{-3} Torr. A monochromator (CS130, Newport) was used to select the wavelength, using a 300 W xenon lamp as the light source. An optical power meter (1936-R, Newport) and Si detector (10UVSI, ICC) were used to measure the light power density. The Si detector was used to cover the wavelength range of 400–1100 nm.

3 Results and Discussion

Figure 1a shows the OM images of the mechanically exfoliated 3R α-In_2Se_3 flakes transferred to a 300-nm-thick SiO_2/Si substrate. AFM was used to determine the heights of the formed layers, as shown in Fig. 1b, and the thickness profiles of the flakes transferred onto SiO_2/Si are plotted in Fig. 1c. We observed that the lowest thickness value of the exfoliated flake was approximately 15.1 nm; other measured thicknesses were approximately 40.2, 72.1, 93.7, and 118.7 nm. Considering that the thickness of a monolayered 3R α-In_2Se_3 is approximately 1 nm [9, 14], the mechanically exfoliated 3R α-In_2Se_3 flakes had 15–120 atomic layers.

Figure 2 shows XRD patterns of the In_2Se_3 that was successfully synthesized as a single 3R phase (α-In_2Se_3, JCPDS #01-034-0455) without impurities. This was demonstrated

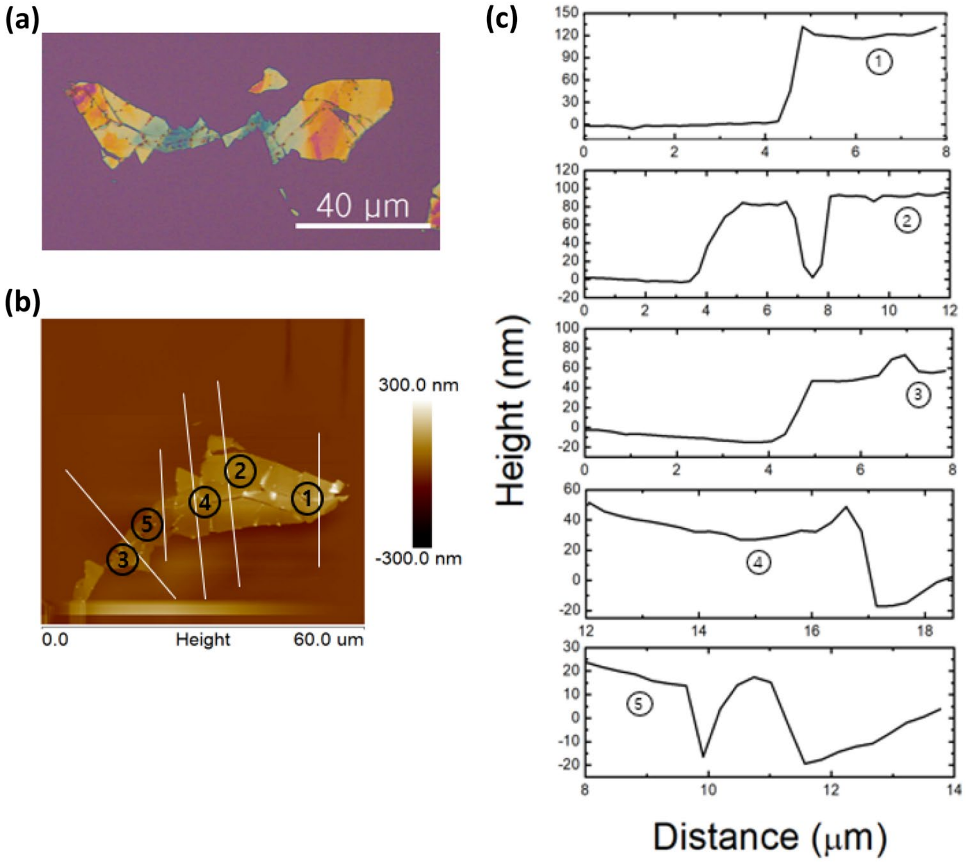

Fig. 1 Topographical characterization of 3R α-In_2Se_3 flake: **a** optical microscopy, **b** topographic AFM image and **c** height-profiles of layers transferred on a SiO_2/Si substrate. The AFM height-profile was obtained along the white line shown in the AFM image. The thinnest film has a layer thickness of approximately 15.1 nm

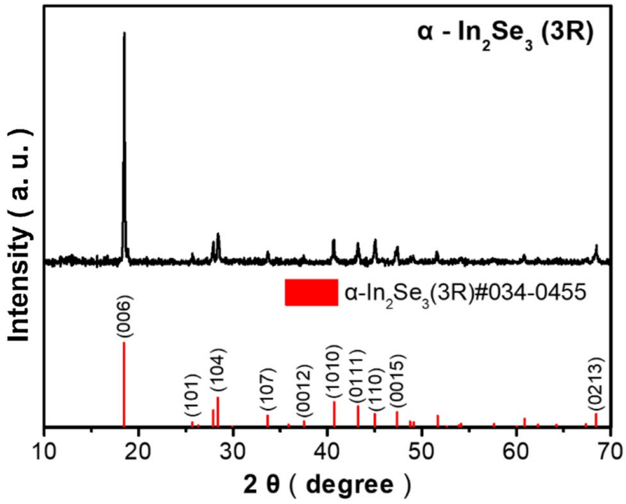

Fig. 2 XRD pattern of the 3R α-In_2Se_3 powder

by comparing the calculated lattice parameters with those in the JCPDS. The lattice parameters *a* and *c* were calculated to be 4.016 and 28.768 Å, respectively, whereas their values in the JCPDS were 4.025 and 28.762 Å, respectively. The conductivity (σ) value of 3R phase α-In_2Se_3 is 12.62 S/cm at 300 K [15, 16].

Figure 3a shows the micro-Raman spectrum of 3R α-In_2Se_3 transferred from the SiO_2/Si substrate at 300 K. Prominent Raman peaks were observed at approximately 90, 102, 180, and 196 cm^{-1} corresponding to the E^2, A_1^1, E^4, and A_1^2 vibration modes, respectively [17]. The thickness dependence of the Raman peak shift is shown in Fig. 3b. According to Fig. 3b, A_1^2 vibration mode tends to shift slightly towards larger wavenumbers as the thickness decreases. The thickest and thinnest Raman peaks were observed at 192.55 cm^{-1} and 196.89 cm^{-1}, respectively. However, A_1^1 and E^4 vibration modes did not depend on layer thickness. As the thickness increased, the A_1^2 peak shifted towards smaller wavenumbers. Zhou et al. observed a similar shift behavior according to the thickness [18]. Compared to its 2H counterpart, the E^2 mode of 3R α-In_2Se_3 appears to be less prominent [10, 14, 18]. Liu et al. confirmed that the intensity ratio between E^2 and A_1^1 modes could be used to distinguish 2H and 3R α-In_2Se_3 [14]. In our study, the 3R α-In_2Se_3 was confirmed because the measured intensity ratio (A_1^1/E^2) was larger than that of the 2H structure.

The PL spectrum obtained at 300 K for thickness values of 15, 40, 72, 94, and 119 nm of the 3R α-In_2Se_3 flakes that were transferred to the SiO_2/Si substrate are shown in Fig. 4a. The PL peaks of thickness of 119 and 15 nm are located at 894.75 and 869.16 nm, respectively, and

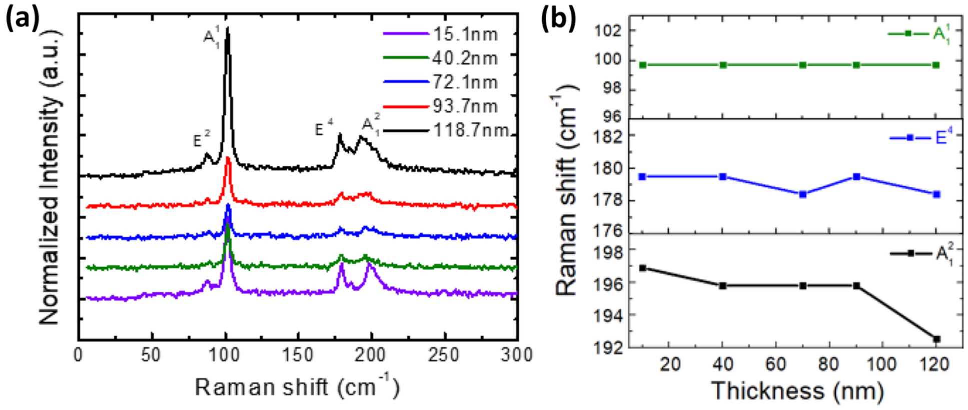

Fig. 3 Optical properties of 3R α-In_2Se_3 flake: **a** normalized micro-Raman spectrum of 15–120 layered 3R α-In_2Se_3 300 K. The main Raman peak observed at approximately 102 cm^{-1} corresponds to the A_1^1 vibration mode. The weaker peaks located at approximately 90 cm^{-1}, 180 cm^{-1}, and 190 cm^{-1} correspond to the E^2, E^4, and A_1^2 vibration modes, respectively. **b** shows the Raman shift versus layer thickness of the A_1^1, E^4, and A_1^2 peaks

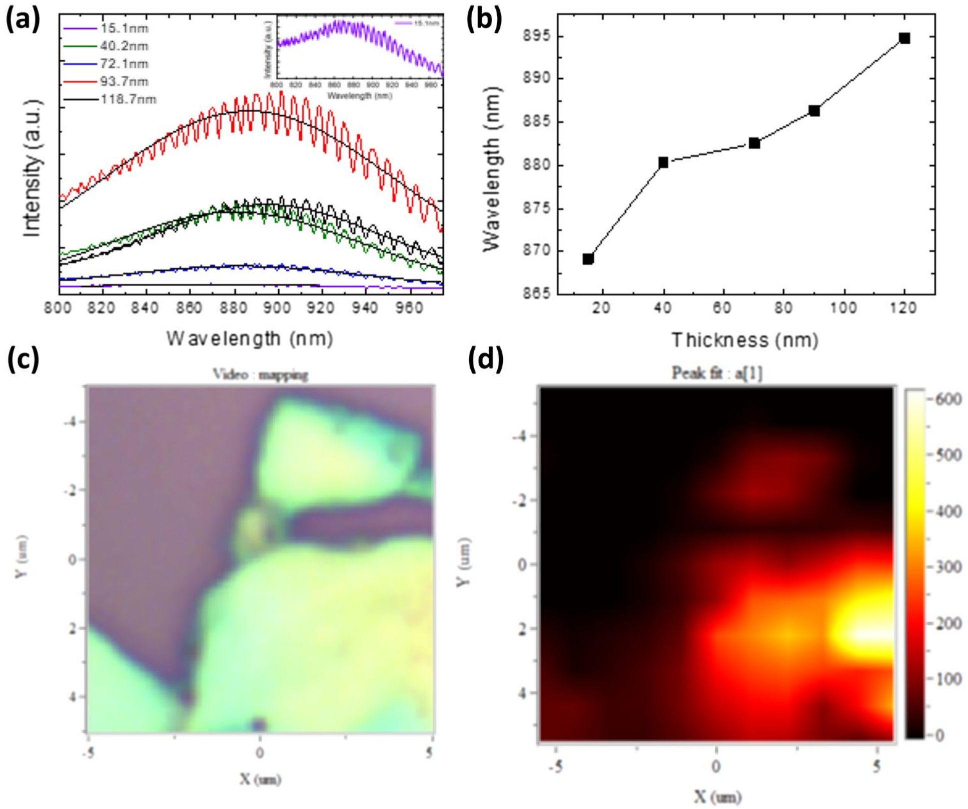

Fig. 4 Optical properties of 3R α-In_2Se_3 flake: **a** PL spectrum of 3R α-In_2Se_3 layers at 300 K. **b** Wavelength versus layer thickness plot indicating the shifting tendency of Raman spectra. **c** Optical image of 3R α-In_2Se_3 flake **d** Normalized PL mapping result of 3R α-In_2Se_3 flake in (**c**)

correspond to 1.39 and 1.43 eV, respectively. As the thickness decreases, the PL emission exhibits a blue shift towards high phonon energies up to 40 meV, which may be due to the quantum confinement effect [6]. A previous study showed the thickness dependence of the PL emission of In_xSe_y that resulted from the combined effect of carrier confinement along the c-axis (z-axis) and on the *xy*-plane [19]. To fully understand the spatial resolution optical properties, we measured PL mapping for 3R α-In_2Se_3 flake (Fig. 4c, d).

Figure 5a shows the OM with surface profiler height-profile (~ 1 µm) and schematic image of the fabricated bulk 3R α-In_2Se_3-based phototransistor. Ti/Au electrodes were deposited as the drain and source on both sides of the device to measure the electrical properties. The length and width of the channel of 3R α-In_2Se_3 are approximately 121.3 and 50.16 µm, respectively. The effective area of the 3R α-In_2Se_3 photodetector was $6.08 \times 10^{-5} cm^2$. The PL spectrum of the bulk 3R α-In_2Se_3 channel shows a peak at 930.14 nm (1.33 eV), as shown in Fig. 5b. Further study including the e-beam lithography fabrication will be necessary to fully understand the thickness dependence optoelectronic properties of 3R a-In_2Se_3 flakes.

The I–V characteristics of the 3R α-In_2Se_3-based phototransistor were measured at 300 K in the dark and under illumination (λ = 750 nm), as shown in Fig. 6a. The photocurrent I_{ph} ($I_{illumination} - I_{dark}$) was measured under

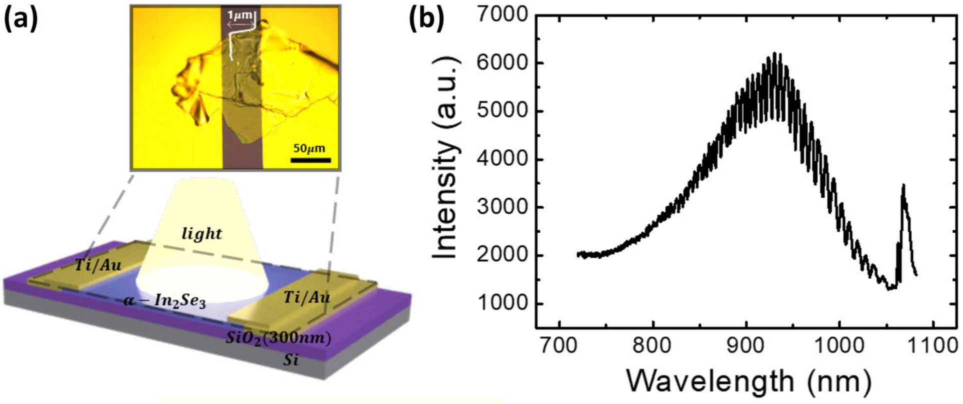

Fig. 5 **a** OM with surface profiler height-profile and schematic images of bulk 3R α-In_2Se_3-based FET manufactured by mechanical exfoliation, respectively. **b** PL spectrum of the 3R α-In_2Se_3-based FET. The bandgap was 1.33 eV, which was measured for comparison in terms of photoresponsivity

illumination (λ = 750 nm). After the bias voltage is applied, an electric field causes the photoexcited electrons and holes in 3R α-In_2Se_3 flow in the opposite directions to generate a photocurrent I_{ph} [20]. The photoresponsivity was calculated using the following equation:

$$R = \frac{I_{ph}}{P_{light} \times A}, \tag{1}$$

where P_{light} and A light power density and the effective area of the α-In_2Se_3 channel, respectively. The calculated results are plotted in In Fig. 6b, which shows the photoresponsivity for each light wavelength. 3R α-In_2Se_3 based phototransistor was detected in a wide spectrum of 300–1050 nm, and the photoresponsivity obtained at a drain voltage of – 10 V at 750 nm at 300 K reached approximately 34,500 A/W. Moreover, we observed a photoresponse from bulk α-In_2Se_3 flakes in the 300–1050 nm region, which correlated well with the band edge transition (PL, 1.33 eV) of the bulk α-In_2Se_3 flakes. A reduction in photoresponsivity at a lower wavelength (< 750 nm) may occur because of a defect in 3R α-In_2Se_3 or a recombination effect of the photogenerated carriers by surface states [21]. In Fig. 6c, the transfer curve of the 3R α-In_2Se_3-based FET shows n-type semiconductor transfer properties, and it was measured at source-drain voltages of 1, 5, 7, and 10 V; the ON/OFF ratios of the α-In_2Se_3-based phototransistor were 1.51, 1.43, 1.62, and 1.84, respectively, and its mobilities were 2.95, 8.87, 16.7, and 24.26 $\mathrm{cm}^2/V \cdot s$, respectively, The mobility (μ) was calculated using the following equation:

$$\mu = \frac{g_m \times L_{channel}}{W_{channel} \times C_g \times V_{ds}}, \tag{2}$$

where, g_m is the transconductance, $L_{channel}$ and $W_{channel}$ are the channel length and width, respectively, and C_g the gate capacitance per unit area. It is well known that α-In_2Se_3 is a ferroelectric semiconductor [13, 22]. When the thickness of the oxide insulator was 300 nm, the voltage applied to the gate did not completely change the polarization of the ferroelectric channel, resulting in partial band bending [13]. Therefore, a clockwise hysteresis loop occurs as expected in the transfer curve measured by the dual-gate voltage sweep, owing to the ferroelectric characteristics (Fig. 6c).

4 Conclusion

In this study, we investigated 3R α-In_2Se_3 flakes that were mechanically exfoliated and transferred onto a SiO_2/Si substrate. Raman and photoluminescence (PL) spectra were measured at room temperature to understand the optical properties of 3R α-In_2Se_3 of various thicknesses (15–120 nm). It was found that the A_1^2 vibration mode, one of the Raman spectrum peaks of 3R α-In_2Se_3, decreases as the thickness increases, and in the PL spectrum, the wavelength exhibits a blue-shift as the thickness decreases. We manufactured a bulk 3R α-In_2Se_3 based field effect transistor (FET) to measure photoresponsivity. The I–V curve was measured under illuminated conditions in the wavelength range of 300–1300 nm, and the photoresponsivity was calculated from the difference between the drain current in the dark condition and the drain current in the illuminated condition. As a result, photoresponsivity of 3R α-In_2Se_3 was detected over a wide wavelength of 300–1050 nm, and it had a distinct photoresponsivity of 34,500 A/W at 750 nm under a drain voltage of – 10 V. From this photoresponsivity peak, it was inferred that it is closely related to the bandgap measured through PL. The transfer curve was measured to confirm the electrical properties of the 3R α-In_2Se_3 nanosheets. Using the transfer curve, t at source-drain voltages of 1, 5, 7, and 10 V, the mobility values were obtained as 2.95, 8.87, 16.7, and 24.26 cm^2/V·s, respectively, and the on/off ratios were 1.51, 1.43, 1.62, and 1.84, respectively. The 3R α-In_2Se_3-based phototransistor exhibited an excellent photoresponsivity. Based on this result, we confirmed that 3R α-In_2Se_3 layers are a promising candidate for optoelectronic applications.

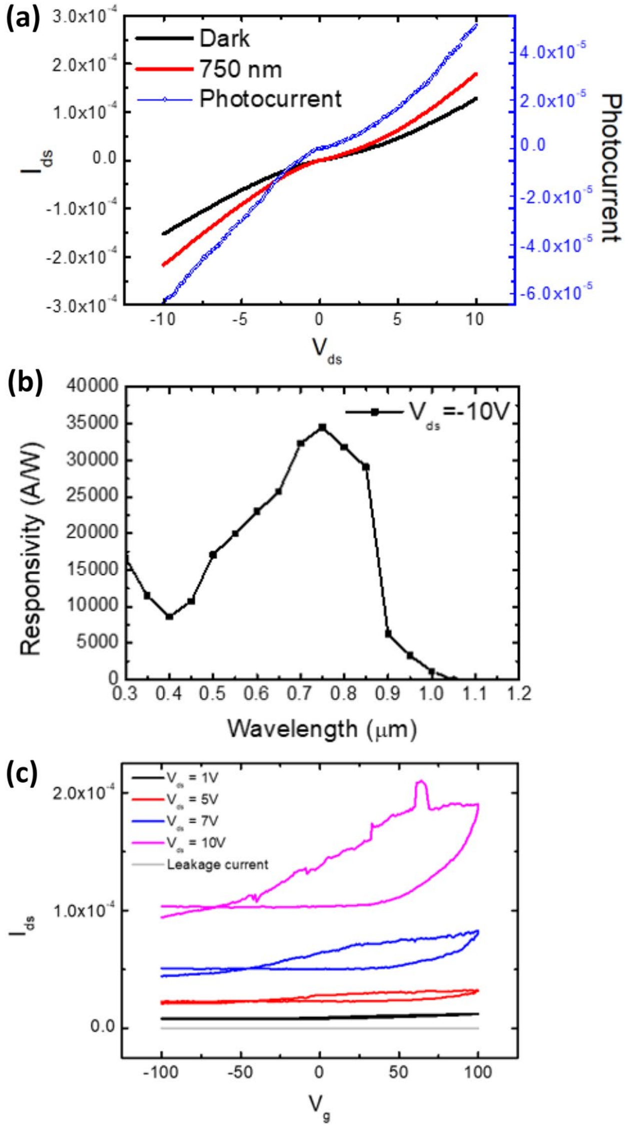

Fig. 6 Optoelectronic properties of 3R α-In_2Se_3: **a** I–V characteristics measured under dark and illuminated conditions (λ = 750 nm), and the measured photocurrent. **b** The photoresponsivity measured at light wavelength in the range of 300–1300 nm. **c** The transfer curves of the 3R α-In_2Se_3-based phototransistor measured using dual gate voltage sweep

Acknowledgements This study was supported by the National Research Foundation of Korea (NRF-2021R1C1C1006147).

Declarations

Conflict of interest The authors declare that they have no confict of interest.

References

1. Rubbert, C., Aslan, B., Heinz, T.F.: Optical properties and band gap of single- and few-layer $MoTe_2$ crystals. Nano Lett. **14**, 6231–6236 (2014)
2. Mak, K.F., Lee, C., Hone, J., Shan, J., Heinz, T.F.: Atomically Thin MoS_2: A new direct-gap semiconductor. Phys. Rev. Lett. **105**, 136805 (2010)
3. Osman, M., Huang, Y., Feng, W., Liu, G., Qiu, Y., Hu, P.: Issue **74**, (2016). Issue in Progess
4. Nakayama, A., Einaga, M., Tanabe, Y., Nakano, S., Ishikawa, F., Yamada, Y.: Structural phase transition in Bi_2Te_3 under high pressure. High Press. Res. **29**, 245–249 (2009)
5. Guo, S., Wang, Y., Zhang, X., Wang, B., Hu: Phase change behavior improvement of Sb_2Te_3 films by Si doping: Raman scattering evidence at elevated temperatures. Z. AIP Adv. **12**, 035002 (2022)
6. Zhou, J., Zeng, Q., Lv, D., Sun, L., Niu, L., Fu, W., Liu, F., Shen, Z., Jin, C., Liu, Z.: Controlled synthesis of high-quality monolayered α-In_2Se_3 via physical vapor deposition. Nano Lett. **15**, 6400–6405 (2015)
7. van Landuyt, J., van Tendeloo, G., Amelinckx, S.: Phase transitions in In_2Se_3 as studied by electron microscopy and electron diffraction. Phys. Stat. Sol. (a) **30**, 299 (1975)
8. Jasinski, J., Swider, W., Washburn, J., Liliental-Weber, Z., Chaiken, A., Nauka, K., Gibson, G.A., Yang, C.C.: Crystal structure of κ-In_2Se_3. Appl. Phys. Lett. **81**, 4356 (2002)
9. Kupers, M., Konze, P.M., Meledin, A., Mayer, J., Englert, U., Wuttig, M., Dronskowski, R.: Controlled crystal growth of indium selenide, In_2Se_3, and the crystal structures of α-In_2Se_3. Inorg. Chem. **57**, 11775–11781 (2018)
10. Xue, F., Zhang, J., Hu, W., Hsu, W.-T., Han, A., Leung, S.-F., Huang, J., Wan, -K., Liu, Y., Zhang, S., He, J., Chang, H., Jr., Wang, W.-H., Zhang, Z.L., Li, X.: Multidirection piezoelectricity in mono- and multilayered hexagonal α-In_2Se_3. ACS Nano **12**, 4976–4983 (2018)
11. Tianyou, Z., Xiaosheng, F., Meiyong, L., Xijin, X., Liang, L., Baodan, L., Yasuo, K., Ying, M., Jiannian, Y., Yoshio, B., Dmitri, G.: Fabrication of high-quality In_2Se_3 nanowire arrays toward high-performance visible-light photodetectors. Nano Lett. **9**(3), 1265–1269 (2009)
12. Wang, J., Yu, H., Hou, C., Zhang: Solution-processable 2D α-In_2Se_3 as an efficient hole transport layer for high-performance and stable polymer solar cells. J. Sol. RRL **4**, 1900428 (2020)
13. Si, M., Saha, A.K., Gao, S., Qiu, G., Qin, J., Duan, Y., Jian, J., Niu, C., Wang, H., Wu, W., Gupta, S.K., Ye, P.: A ferroelectric semiconductor field-effect transistor. Nat. Electron. **2**, 580–586 (2019)
14. Liu, L., Dong, J., Huang, J., Nie, A., Zhai, K., Xiang, J., Wang, B., Wen, F., Mu, C., Zhao, Z., Gong, Y., Tian, Y., Liu: Atomically resolving polymorphs and crystal structures of In_2Se_3. Z. Chem. Mater. **31**, 10143–10149 (2019)
15. Chen, Y.X., Li, F., Wang, W., Zheng, Z., Luo, J., Fan, P., Takeuchi, T.: Optimization of thermoelectric properties achieved in Cu doped β-In_2S_3 bulks. J. Alloys Compd. **782**, 641 (2019)
16. Park., O., Lee, S.W., Kim, S.: Thermoelectric properties of Si-doped In_2Se_3 polycrystalline alloys. Ceram. **5**, 281 (2022)
17. Solanke, S.V., Soman, R., Rangarajan, M., Raghavan, S., Nath, D.N.: UV/near-IR dual band photodetector based on p-GaN/α-In_2Se_3 heterojunction. Sens. Actuators A **317**, 112455 (2021)
18. Zhou, Y., Wu, D., Zhu, Y., Cho, Y., He, Q., Yang, X., Herrera, K., Chu, Z., Han, Y., Downer, M.C., Peng, H., Lai, K.: Out-of-plane piezoelectricity and ferroelectricity in layered α-In_2Se_3 nanoflakes. Nano Lett. **17**, 5508–5513 (2017)
19. Mudd, G.W., Svatek, S.A., Ren, T., Patanè, A., Makarovsky, O., Eaves, L., Beton, P.H., Kovalyuk, Z.D., Lashkarev, G.V.,

Kudrynskyi, Z.R., Dmitriev, A.: Tuning the bandgap of exfoliated InSe nanosheets by quantum confinement. I Adv. Mater. **25**, 5714–5718 (2013)

20. Balakrishnan, N., Staddon, C.R., Smith, E.F., Stec, J., Gay, D., Mudd, G.W., Makarovsky, O., Kudrynskyi, Z.R., Kovalyuk, Z.D., Eaves, L.: Quantum confinement and photoresponsivity of β-In_2Se_3 nanosheets grown by physical vapour transport. 2D Mater. **3**, 025030 (2016)
21. Ho, C.-H., Lai, X.-R., Chuang, C.-A., Kuo, W.-L., Tiong, K.-K.: The study of optical properties of III_2-IV_3 defect semiconductor group compounds Ga_2S_3, Ga_2Se_3, In_2S_3, and In_2Se_3. Adv. Photonics Res. **2**, 2000110 (2021)
22. Ding, W., Zhu, J., Wang, Z., Gao, Y., Xiao, D., Gu, Y., Zhang, Z., Zhu, W.: Prediction of intrinsic two-dimensional ferroelectrics in In_2Se_3 and other III_2-VI_3 van der Waals materials. Nat. Commun. **8**, 14956 (2017)